

Evidence of Registry at the Interface during Inorganic Nucleation at an Organic Template

Jan Kmetko,* Chungjong Yu, Guennadi Evmenenko, Sumit Kewalramani, and Pulak Dutta†

Department of Physics and Astronomy, Northwestern University, Evanston, Illinois 60208

(Received 18 June 2002; published 15 October 2002)

In situ synchrotron x-ray diffraction studies of the nucleation of barium fluoride from supersaturated solutions, at fatty-acid monolayer templates, reveal a commensurate relationship between the interfacial lattices of the organic molecules and the inorganic atoms. At the onset of growth, the barium fluoride layer is very thin and the lateral unit cell is contracted by as much as 4%; at the same time the organic molecules tilt, expanding the organic unit cell. This flexibility is what allows the lattice parameters to be commensurate. Such registry is expected to play an important precursor role in controlled biomineralization and organic-matrix-mediated materials synthesis.

DOI: 10.1103/PhysRevLett.89.186102

PACS numbers: 68.55.-a, 61.10.Eq, 68.18.-g, 81.10.Dn

In many biologically controlled (“organic-matrix-mediated”) processes, macromolecular substrates direct the nucleation of crystalline biological components, for example, of skeletal materials [1–4]. Langmuir monolayers are often used as simple models of biomineralization [5–7]; they can guide the growth of oriented crystals of specific structure, size, and morphology. Although the assembly of nuclei is assumed to proceed through the process of molecular recognition at the interface, this assumption has so far been supported only by circumstantial evidence.

Such face-selective nucleation presumably stems from a match between the interfacial lattices of the organic molecules and the inorganic atoms. Although previous grazing incidence diffraction (GID) studies on dilute solutions of aqueous salts [8–10] found diffraction spots from superlattices, these peaks could not be assigned to any known structures of bulk compounds. Such salts, for example, manganese, magnesium, cadmium, or lead chloride, either did not grow at the interface beyond the first monolayer or grew as nonoriented powders at supersaturated concentrations. GID studies have also been done on oriented crystal growth of glycine under Langmuir monolayers of α -amino acids [11], and on growth of oriented ice under alcohol monolayers [12]. When nucleating glycine crystals, the evidence for epitaxy was that the monolayer of α -amino acid molecules of a single handedness selectively induced formation of the enantiomeric crystal face composed of molecules of the opposite handedness. In the case of ice nucleation, an approximate (within 0.5 Å) lattice match between arrangements of the oxygen atoms in the layer of hexagonal ice and of the oxygen atoms in the alcohol molecules was observed. In either case, no precise linear relationship between the basis vectors of the organic and inorganic lattices has been determined.

In a multitude of other, nonstructural studies [13–24], it is assumed that the “hard” mineral has the same structure at the interface as it does in the bulk, and that the “soft” monolayer matrix at the surface of a concen-

trated solution has the same lattice spacings as have been reported for the monolayer on pure water. With these assumptions, an approximate commensurate relationship is identified. Such efforts are entirely reasonable in the absence of *in situ* evidence. However, in our studies we find that neither the organic nor the inorganic lattice is rigid; they exert a mutual influence on each other to achieve precise registry at the initial stage of growth.

We spread Langmuir monolayers of heneicosanoic acid on supersaturated solutions of barium fluoride at just above zero pressure and 25 °C. The BaF₂ solutions were prepared at various concentrations from 3 mM (saturated) to 14 mM by mixing appropriate stoichiometric amounts of barium chloride and ammonium fluoride, a method similar to that in [21]. The pH was adjusted to 8 with sodium hydroxide for all samples. The samples were irradiated by a beam of $\lambda = 1.5491$ Å in the GID geometry; details of the setup can be found in [25]. The crossed soller slits in front of the detector defined a horizontal resolution $K_{\parallel} \sim 0.01$ Å⁻¹ full width at half maximum (FWHM) and a vertical resolution $K_{\perp} \sim 0.05$ Å⁻¹ FWHM. Because the monolayer is a powder within the plane, it is not possible to determine the direction of the in-plane momentum transfer vector K_{\parallel} , only its magnitude. The vertical component K_{\perp} can be measured separately.

At low barium ion concentrations, only one organic in-plane peak corresponding to the untilted *LS* phase is seen. It has been reported in previous studies [9] that dilute barium ions at 10 °C induce the high-pressure *S* phase in the monolayer; similarly, in our present experiments, performed at 25 °C, they compress the monolayer to the high-pressure *LS* phase even at zero pressure. The spacings of the *LS* phase are not commensurate with those of BaF₂. As the solution concentration increases, the organic molecules phase separate to form an entirely new coexisting phase. Three additional peaks appear, one in plane and two out of plane [Fig. 1(a)].

In this new phase, the molecules are tilted at 29° to the surface normal; the new primitive unit cell has lattice

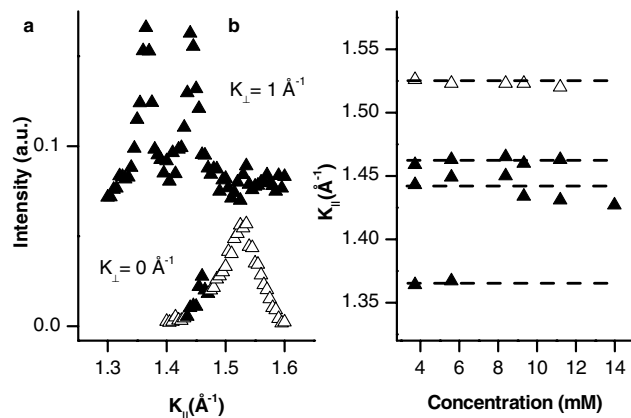


FIG. 1. Reorganization of heneicosanoic acid monolayers. At low concentrations, only the LS peak (Δ) corresponding to an untilted structure is seen. (a) At the saturated concentration ($= 3.7$ mM), one in-plane and two out-of-plane organic peaks (\blacktriangle) can also be seen, indicating a coexisting tilted structure. (b) At higher concentrations, the organic peak positions do not change with concentration. (The position of the peak at $K_{\parallel} \sim 1.36$ \AA^{-1} is smeared out by the growing $\{111\}$ peak of BaF_2 and cannot be accurately determined at higher concentrations.)

parameters $|\mathbf{a}_0| = 5.249$ \AA , $|\mathbf{b}_0| = 5.188$ \AA , $\gamma = 124.0^\circ$, and area = 22.59 $\text{\AA}^2/\text{molecule}$. These three peaks can be identified as organic because the diffraction peaks have a width in the z direction (Bragg rod width) consistent with the thickness of the fatty-acid monolayer. Moreover, the positions of these peaks do not change as a function of salt concentrations in the subphase [Fig. 1(b)]. However, the peak intensities change, indicating that the fraction of the monolayer in the new organic phase is increasing at the expense of the LS phase.

In contrast, the structure of BaF_2 at the interface depends on solution concentration. The inorganic peaks correspond to a cubic phase with lattice spacings not far from that of bulk BaF_2 , but at low concentrations the peak positions are higher than the bulk positions [Fig. 2(a)]. Since other $\{hk0\}$ peak positions also depend on concentration [Fig. 2(b)], the $\langle 100 \rangle$ face of the mineral changes in size, but always remains a square. In other words, the lattice of the mineral is strained, with the horizontal unit-cell spacing contracted from its bulk value of 6.20 \AA by as much as 4%. The vertical spacing cannot be determined with sufficient precision [26]. Such strain can occur in thin films [27], and, indeed, the broad Bragg rods of the $\{hk0\}$ peaks indicate that the inorganic layer is less than 14 \AA thick when the solution concentration is 5.6 mM [Fig. 3(a)]. The lateral size of fatty-acid domains and the BaF_2 crystallites can be estimated from the widths of the respective peaks. The average size of the inorganic domains increases from ~ 100 \AA to ~ 250 \AA as the concentration increases from 5.6 to 14.0 mM. The size of the organic domains is ~ 250 \AA and does not change.

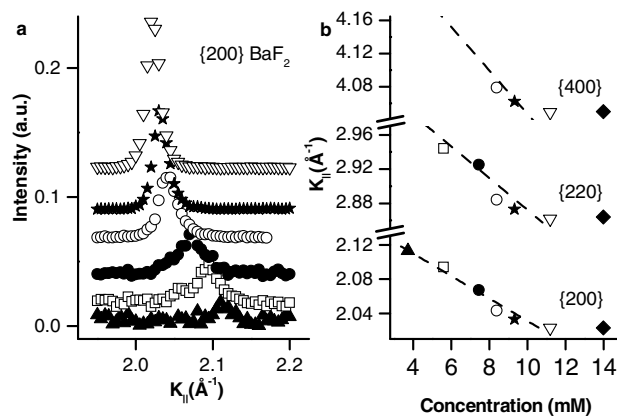


FIG. 2. Strain relaxation in barium fluoride at the mineral-matrix interface. (a) A representative $\{200\}$ diffraction peak “shifts” as a function of concentration. The following symbols denote the concentration of the salt in the subphase (in mM): \blacklozenge , 14.0 ; ∇ , 11.2 ; \star , 9.3 ; \circ , 8.4 ; \bullet , 7.5 ; \square , 5.6 ; \blacktriangle , 3.7 . (b) Other $\{hk0\}$ peaks “shift” positions as well. The line through the $\{200\}$ data is a linear fit; the lines through the $\{220\}$ and $\{400\}$ data are calculated from the $\{200\}$ fit. At lower concentrations, some higher-order peaks are too weak to observe.

The strain in the interfacial structure of BaF_2 decreases as the solution concentration increases (Fig. 2), until the lattice spacing reaches the known bulk value at > 11 mM concentration. (We also see the $\{111\}$, $\{220\}$, $\{311\}$, $\{400\}$, and $\{331\}$ peaks of bulk BaF_2 .) At higher concentrations, the diffracted intensity is not distributed along Bragg rods but rather along “Debye” rings [Fig. 3(b)]. The mineral has grown from a thin layer to slightly misoriented bulk crystallites. Intensity variations along $\{hk0\}$ rings have their maxima at $K_{\perp} \sim 0$ \AA^{-1} (in the plane of water), and intensities on the $\{hk1\}$ rings reach maximum at $K_{\perp} \sim 1$ \AA^{-1} ; from that, it follows that the $\langle 100 \rangle$ face of bulk barium fluoride lies parallel to the plane of the matrix. We do not see evidence of other epitaxial orientations or any unoriented crystallites. Based on the intensity variations along the rings, the extent of misorientation is only 2.5° at 11.2 mM. It should be noted that either without any monolayer (no template) or under a monolayer of heneicosanol (neutral headgroups), barium fluoride and barium chloride fluoride nucleate at the interface as nonoriented crystallites.

The effects observed as a function of concentration are also observed by varying the temperature. Crystallites should grow with decreasing temperature because the solubility of barium fluoride decreases, and the crystallites should shrink with increasing temperature because they partially redissolve. When the sample is cooled from 25 to 10 $^\circ\text{C}$ at a slightly oversaturated concentration, the BaF_2 spacings expand by 0.9% . The process is reversible; when the sample is heated back to 25 $^\circ\text{C}$, the spacings contract by almost the same percentage. These results are

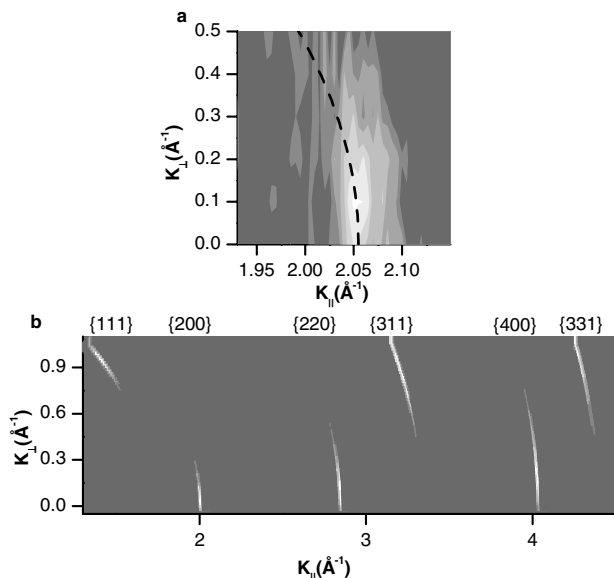


FIG. 3. The growth of barium fluoride. (a) At a low concentration (5.6 mM), the diffracted intensity of the {200} diffraction spot is “stretched” in the out-of-plane direction along a Bragg rod. The intensity would follow a “Debye ring” (dashed line) if the mineral were a powder. (b) At higher concentrations (11.2 mM), the diffracted intensity is peaked along the Debye rings. The positions of the “hot spots” indicate that the crystallites are preferentially oriented with the $\langle 100 \rangle$ face parallel to the plane of the water surface. This image was not obtained by an image plate or similar device, but was reconstructed from detector scans.

consistent with the expected inverse relationship between strain and film thickness. To ascertain that the “peak shifting” is not an artifact of a chemical reaction, for example, of incorporating either chlorine or ammonium ions into the interfacial structure (Vegard’s law), we have also prepared the supersaturated solution of BaF_2 by mixing stoichiometric amounts of hydrofluoric acid with barium hydroxide. This method of sample preparation, used only on occasion because of safety concerns when working with hydrofluoric acid, reproduced the trends reported here exactly.

Although scattering from the BaF_2 structure is too weak to observe at concentrations below 4 mM, we can extrapolate to zero concentrations to determine the structure at the earliest stage. A linear fit to the trend of the lattice contraction in Fig. 2(b) intercepts the K_{\parallel} axis at 2.16\AA^{-1} . The corresponding real-space parameters of the face-centered-square unit cell (the face of the cubic BaF_2) are $|\mathbf{a}_i| = |\mathbf{b}_i| = 5.82 \text{\AA}$, and the area of the face is 33.85\AA^2 . The area of the organic unit cell [from data in Fig. 1(a)] is 22.59\AA^2 . The ratio of these numbers is 1.50, which strongly suggests that these structures are epitaxial. Indeed, the lattices are commensurate; i.e., they share a common supercell. The supercell basis vectors ($\mathbf{a}_s, \mathbf{b}_s$) can be defined in terms of either the organic ($\mathbf{a}_o, \mathbf{b}_o$) or

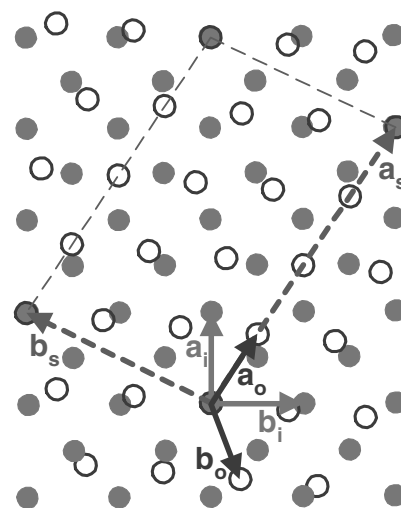


FIG. 4. Real space lattices of the fatty-acid headgroups (\circ) and barium atoms (\bullet) of the $\langle 100 \rangle$ face of barium fluoride. The lattices are commensurate because they share a common supercell (outlined by the dashed line). See text for the definition of relationships among the supercell ($\mathbf{a}_s, \mathbf{b}_s$), organic ($\mathbf{a}_o, \mathbf{b}_o$), and inorganic ($\mathbf{a}_i, \mathbf{b}_i$) basis vectors. The relative translation of the two lattices is arbitrary.

inorganic ($\mathbf{a}_i, \mathbf{b}_i$) basis vectors:

$$\begin{aligned} \mathbf{a}_s &= 4\mathbf{a}_o = 3\mathbf{a}_i + 2\mathbf{b}_i, \\ \mathbf{b}_s &= -2\mathbf{a}_o - 3\mathbf{b}_o = \mathbf{a}_i - 2\mathbf{b}_i. \end{aligned}$$

These relationships are accurate to better than 0.1%. The real-space lattices are shown in Fig. 4.

These results indicate that both the organic matrix and the nucleating structure undergo rearrangements to allow the atomic planes of the hard mineral to continue those of the soft organic substrate. Not only can an exact relationship (as opposed to a postulated approximate relationship) exist between parameters of the organic and inorganic lattices, but also the coincidence of parameters allows selective nucleation—of the several possible species (barium fluoride, barium chloride fluoride, barium hydroxide) and crystallographic orientations, the fatty-acid monolayer exclusively selects out crystals of barium fluoride with well-oriented $\langle 100 \rangle$ crystallographic faces for nucleation. An exact coincidence between the structures of different materials is normally rare, but it can occur if the interfacial lattices deform. Strained epitaxial growth is well known in thin film studies under ultrahigh vacuum, but we have now seen that it can happen in template-directed growth from solution as well.

This work was supported by the U.S. Department of Energy under Grant No. DE-FG02-84ER45125. It was performed at beam line X14 of the National Synchrotron Light Source and at Sector I (SRI-CAT) of

the Advanced Photon Source. We thank Dr. J. Bai for his valuable assistance at X14, and Dr. J. Wang and Dr. S. Narayanan for their help at SRI-CAT.

*Present address: Department of Physics, Cornell University, Ithaca, NY 14853.

†Electronic address: pdudda@northwestern.edu

- [1] L. Addadi, E. Beniash, and S. Weiner, in *Supramolecular Organization and Materials Design*, edited by W. Jones and C. Rao (Cambridge University Press, Cambridge, U.K., 2002), p. 1.
- [2] S. Mann, in *Inorganic Materials*, edited by D.W. Bruce and D. O'Hare (Wiley, Chichester, U.K., 1992), p. 238.
- [3] S. Mann, *Nature (London)* **365**, 499 (1993).
- [4] S. Mann, D.D. Archibald, J.M. Didymus, T. Douglas, B.R. Heywood, F.C. Meldrum, and N.J. Reeves, *Science* **261**, 1286 (1993).
- [5] M. Lahav and L. Leiserowitz, *J. Phys. D* **26**, B22 (1993).
- [6] H. Rapaport, I. Kuzmenko, M. Berfeld, K. Kjaer, J. Als-Nielsen, R. Popovitz-Biro, I. Weissbuch, M. Lahav, and L. Leiserowitz, *J. Phys. Chem. B* **104**, 1399 (2000).
- [7] I. Weissbuch, R. Popovitz-Biro, M. Lahav, and L. Leiserowitz, *Acta Crystallogr. Sect. B* **51**, 115 (1995).
- [8] F. Leveiller, C. Bohm, D. Jacquemain, H. Mohwald, L. Leiserowitz, K. Kjaer, and J. Als-Nielsen, *Langmuir* **10**, 819 (1994).
- [9] J. Kmetko, A. Datta, G. Evmenenko, and P. Dutta, *J. Phys. Chem. B* **105**, 10818 (2001).
- [10] J. Kmetko, A. Datta, G. Evmenenko, M. K. Durbin, A. G. Richter, and P. Dutta, *Langmuir* **17**, 4697 (2001).
- [11] I. Weissbuch, M. Berfeld, W. Bouwman, K. Kjaer, J. Als-Nielsen, M. Lahav, and L. Leiserowitz, *J. Am. Chem. Soc.* **119**, 933 (1997).
- [12] J. Majewski, R. Popovitz-Biro, K. Kjaer, J. Als-Nielsen, M. Lahav, and L. Leiserowitz, *J. Phys. Chem.* **98**, 4087 (1994).
- [13] R. Backov, C. M. Lee, S. R. Khan, C. Mingotaud, G. E. Fanucci, and D. R. Talham, *Langmuir* **16**, 6013 (2000).
- [14] L. M. Frostman and M. D. Ward, *Langmuir* **13**, 330 (1997).
- [15] B. R. Heywood and S. Mann, *Adv. Mater.* **4**, 278 (1992).
- [16] B. R. Heywood and S. Mann, *Langmuir* **8**, 1492 (1992).
- [17] B. R. Heywood and S. Mann, *J. Am. Chem. Soc.* **114**, 4681 (1992).
- [18] B. R. Heywood and S. Mann, *Chem. Mater.* **6**, 311 (1994).
- [19] B. Li, Y. Liu, N. Lu, J. Yu, Y. Bai, W. Pang, and R. Xu, *Langmuir* **15**, 4837 (1999).
- [20] L. Lu, H. Cui, W. Li, H. Zhang, and S. Xi, *J. Mater. Res.* **16**, 2415 (2001).
- [21] J. B. Walker, B. R. Heywood, and S. Mann, *J. Mater. Chem.* **1**, 889 (1991).
- [22] J. Yang, F. C. Meldrum, and J. H. Fendler, *J. Phys. Chem.* **99**, 5500 (1995).
- [23] J. Yang and J. H. Fendler, *J. Phys. Chem.* **99**, 5505 (1995).
- [24] X. Zhao, J. Yang, L. McCormick, and J. Fendler, *J. Phys. Chem.* **96**, 9933 (1992).
- [25] S. Barton, B. Thomas, E. Flom, S. Rice, B. Lin, J. Peng, J. Ketteron, and P. Dutta, *J. Chem. Phys.* **89**, 2257 (1988).
- [26] At low concentrations, the inorganic layer is thin, and thus the diffraction peaks are smeared along the z direction [Fig. 3(a)]. At higher concentrations the peaks are again smeared along "Debye rings" [Fig. 3(b)]. In either case the spacings in the z direction cannot be measured as precisely as those in the horizontal plane.
- [27] A. A. Chernov, *Modern Crystallography III: Crystal Growth*, Solid-State Sciences Vol. 36 (Springer-Verlag, New York, 1980).